AUT Journal of Mechanical Engineering

AUT J. Mech. Eng., 3(2) (2019) 235-242
DOI: 10.22060/ajme.2019.14844.5748

Mixed-Mode Fracture Analysis of a Functionally Graded Layer with Clamped Longitudinal Edges

A.M. Baghestani[1*], S.J. Fariborz[2]

[1] Department of Mechanical Engineering, Babol Noshirvani University of Technology, Babol, Iran
[2] Department of Mechanical Engineering, Amirkabir University of Technology, Tehran, Iran

ABSTRACT: Properties of functionally graded materials as nonhomogeneous solids with gradually varied composition make them suitable for many applications, such as coating in interfacial zones. The present study investigates the plane elasticity problem for an isotropic functionally graded material layer containing multiple cracks using the distributed dislocation technique. The layer has a finite thickness and infinite length where it's top and bottom surfaces are fixed. The elastic modulus of the medium is assumed to vary exponentially in the thickness direction. The Fourier integral transform method is used to obtain the stress fields caused by an edge dislocation in the layer. The stress components exhibit familiar Cauchy as well as logarithmic singularity at the dislocation position. In fact, the dislocation solution in this study is primarily employed to derive a set of integral equations to analyze cracks with arbitrary configuration. The numerical solution of these equations yields dislocation densities on a crack surface which is used to compute the crack stress intensity factors. Then after validating the formulation for homogenous case, several configurations of embedded cracks such as a rotating crack, a stationary horizontal and a rotating crack, two fixed vertical and a horizontal crack with variable location are investigated. Moreover, effects of important parameters on stress intensity factors such as crack geometries, material non-homogeneity and boundary condition are studied.

Review History:
Received: 16 August 2018
Revised: 18 December 2018
Accepted: 27 December 2018
Available Online: 1 January 2019

Keywords:
Functionally graded material layer
Mixed-mode
Fixed boundary
Multiple cracks

1- Introduction

Functionally Graded Materials (FGMs) are usually a mixture of two distinct materials whose properties vary gradually in a specific spatial direction. Most FGMs are made of ceramics and metals to create high temperature resistance and great toughness at the same time. The accurate stress analysis of a FGM structure as a safety-critical structure is the first step in the design process. The task is more highlighted in structures with sharp geometric discontinuities such as cracks. Recently, considerable amount of analytical studies are focusing on fracture behavior of FGMs. However due to intrinsic complexity of the problem, most of studies are limited to infinite or semi-infinite domains, special crack orientations or a single crack in the media. A brief review of studies concerning analytical fracture analysis of FGM media under static loading is presented here. Erdogan and wu [1] considered a FGM layer containing an embedded crack perpendicular to its boundaries under three different mechanical loading. Kadioglu et al. [2] solved the problem of a FGM layer attached to an elastic foundation weakened by a vertical crack. Jin and Paulino [3] studied a horizontal crack in a visco-elastic FGM strip subjected to tensile loading. A Functionally Graded (FG) coating-substrate structure with an embedded or edge crack perpendicular to the interface was investigated by Guo et al. [4]. Long and Delale [5] obtained modes I and II Stress Intensity Factors (SIFs) of an arbitrary oriented embedded crack in a FGM layer. They also in a separate study [6] extended their efforts on analyzing a FGM layer bonded to a homogenous half-plane weakened by a crack. El-Borgi et al. [7] analyzed a vertical edge crack in a graded coating bonded to a homogenous substrate. Dag et al. [8] considered an orthotropic FGM layer weakened by an embedded crack under mechanical and thermal loading. They solved the problem using a numerical enriched finite element as well as an analytical approach and then compared the results. Zhong and Cheng [9] employed a multi-layered model to analyze arbitrary variations of material properties of a FGM strip with a single horizontal crack. Two bonded dissimilar FG strips containing an interface crack was studied by Cheng et al. [10]. The problem of a horizontal crack in an orthotropic FGM layer bonded to a semi-infinite homogeneous medium was addressed by Ben-Romdhane et al. [11]. Petrova and schmauder [12] considered crack interaction problem in a FG coating on a homogenous substrate. The problem was formulated as singular integral equations and effects of different parameters on SIFs were studied. Guo et al. [13] developed a pieswise-exponential model to analyze the mixed-mode interface crack problem of FGM coating structure. In the aforementioned studies, mainly a single crack problem is investigated and their methods may not be used to handle interaction between multiple cracks with arbitrary arrangement. Recently, Monfared et al. [14] analyzed an orthotropic FGM layer containing multiple cracks. They used Distributed Dislocation Technique (DDT) and Airy stress function method to solve the problem. They considered free-free boundary conditions for the layer.

The main objective of the present study is to apply DDT for the stress analysis of multiple cracks in a FGM layer with fixed edges. Moreover, Navier equations are solved directly which allows analyzing layers with different boundary conditions more easily. The method is also capable of handling curved cracks. However, crack closing is not allowed. The edge dislocation problem in the FG layer is solved by integral

Corresponding author, E-mail: am.baghestani@nit.ac.ir

transform method. By means of DDT, the dislocation solution is used to formulate singular integral equations for a FG layer weakened by multiple embedded cracks. Then after validating the formulation, effects of nonhomogeneity parameter and crack configurations on the SIFs are studied. The presented results could be used as the initial step to fracture analysis of FGM layers that are used as interfacial layer in different applications.

2- Dislocation Solution

We consider a FGM layer with thickness h, Fig.1. The coordinate system is such that $|x|<\infty$, and $0<y<h$. Top and bottom surfaces of layer are fixed. Gradation of the material properties of the layer, except for the Poisson's ratio, ν, which is assumed constant [1], is in the y-direction. In two-dimensional elasticity, the equilibrium equations in terms of in-plane displacement components $u(x,y)$ and $v(x,y)$ in the x- and y-directions, respectively, are as follows

$$\begin{aligned}&\frac{\kappa+1}{\kappa-1}\frac{\partial^2 u}{\partial x^2}+\frac{2}{\kappa-1}\frac{\partial^2 v}{\partial x\partial y}+\frac{\partial^2 u}{\partial y^2}\\&+\frac{1}{\mu(y)}\frac{\partial\mu(y)}{\partial y}\left(\frac{\partial u}{\partial y}+\frac{\partial v}{\partial x}\right)=0\\&\frac{\kappa+1}{\kappa-1}\frac{\partial^2 v}{\partial y^2}+\frac{2}{\kappa-1}\frac{\partial^2 u}{\partial x\partial y}+\frac{\partial^2 v}{\partial x^2}\\&+\frac{1}{\mu(y)}\frac{\partial\mu(y)}{\partial y}\left(\frac{\kappa+1}{\kappa-1}\frac{\partial v}{\partial y}+\frac{3-\kappa}{\kappa-1}\frac{\partial u}{\partial x}\right)=0\end{aligned}\tag{1}$$

where $\mu(y)$ and κ are elastic shear modulus and Kolosov constant of the medium which is $\kappa=3-4\nu$ for plane strain and $\kappa=(3-\nu)/(1+\nu)$ for plane stress conditions. As commonly used by fracture community [1,2], [4-8], the shear modulus of the FGM layer is assumed to vary exponentially as

$$\mu(y)=\mu_0 e^{2\beta y}\tag{2}$$

It is also shown that under mechanical loading, the effect of different functions on estimating property distributions of FGMs, on the SIFs is relatively small [15]. Eq. (1), in view of Eq. (2) reduce to

$$\begin{aligned}&\frac{\kappa+1}{\kappa-1}\frac{\partial^2 u}{\partial x^2}+\frac{2}{\kappa-1}\frac{\partial^2 v}{\partial x\partial y}+\frac{\partial^2 u}{\partial y^2}+2\beta\left(\frac{\partial u}{\partial y}+\frac{\partial v}{\partial x}\right)=0\\&\frac{\kappa+1}{\kappa-1}\frac{\partial^2 v}{\partial y^2}+\frac{2}{\kappa-1}\frac{\partial^2 u}{\partial x\partial y}+\frac{\partial^2 v}{\partial x^2}+2\beta\left(\frac{\kappa+1}{\kappa-1}\frac{\partial v}{\partial y}+\frac{3-\kappa}{\kappa-1}\frac{\partial u}{\partial x}\right)=0\end{aligned}\tag{3}$$

The layer contains an edge dislocation located at (ξ,η) where dislocation cut is $x>\xi$, Fig. 1. In the solution of static crack problems by distributed dislocation technique, the orientation of dislocation cut is immaterial. The equations identifying the edge dislocation are

$$\begin{aligned}&u\left(x,\eta^+\right)-u\left(x,\eta^-\right)=B_x H\left(x-\xi\right)\\&v\left(x,\eta^+\right)-v\left(x,\eta^-\right)=B_y H\left(x-\xi\right)\\&\sigma_{xy}\left(x,\eta^+\right)=\sigma_{xy}\left(x,\eta^-\right)\\&\sigma_y\left(x,\eta^+\right)=\sigma_y\left(x,\eta^-\right)\end{aligned}\tag{4}$$

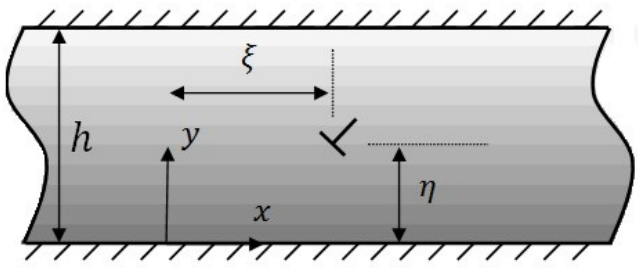

Fig. 1. Schematic view of a FG layer weakened by an edge dislocation

where B_x, B_y are the components of Burgers vector identifying glide and climb of the edge dislocation respectively and $H(x)$ is the Heaviside step function. The layer is assumed as clamped on longitudinal edges, thus boundary conditions are

$$\begin{aligned}&u(x,0)=v(x,0)=0\\&u(x,h)=v(x,h)=0\end{aligned}\tag{5}$$

Eq. (3) with boundary conditions (Eqs. (4) and (5)) is solved by means of the complex Fourier transform, F, [16], with respect to variable x to Eq. (3), $[\bar{u}(\alpha,y),\bar{v}(\alpha,y)]=F[u(x,y),v(x,y);\alpha]$. Assuming that stress components decay in a sufficiently-rapid manner as $|x|\to\infty$, results in

$$\begin{aligned}&\frac{d^2\bar{u}}{dy^2}+2\beta\frac{d\bar{u}}{dy}-\frac{2i\alpha}{\kappa-1}\frac{d\bar{v}}{dy}-2\alpha\beta i\bar{v}-\alpha^2\frac{\kappa+1}{\kappa-1}\bar{u}=0\\&\frac{d^2\bar{v}}{dy^2}+2\beta\frac{d\bar{v}}{dy}-\frac{2i\alpha}{\kappa+1}\frac{d\bar{u}}{dy}-2\alpha\beta i\frac{3-\kappa}{\kappa+1}\bar{u}-\alpha^2\frac{\kappa-1}{\kappa+1}\bar{v}=0\end{aligned}\tag{6}$$

The solution to Eq. (6) may be expressed as

$$\begin{aligned}&\bar{u}_k(\alpha,y)=\left(\pi\delta(\alpha)+\frac{i}{\alpha}\right)e^{-\beta(y-\eta)+i\alpha\xi}\sum_{j=1}^{4}A_{kj}e^{-S_j y},\\&\bar{v}_k(\alpha,y)=\left(\pi\delta(\alpha)+\frac{i}{\alpha}\right)e^{-\beta(y-\eta)+i\alpha\xi}\sum_{j=1}^{4}\frac{m_j}{i\alpha}A_{kj}e^{-S_j y}\\&k\in\{1,2\}\end{aligned}\tag{7}$$

where $\delta(.)$ is the Dirac delta function and

$$\begin{aligned}&S_1=-S_2=\sqrt{\beta^2+\alpha^2+i\sqrt{4\alpha^2\beta^2(3-\kappa)/(\kappa+1)}},\\&S_3=-S_4=\sqrt{\beta^2+\alpha^2-i\sqrt{4\alpha^2\beta^2(3-\kappa)/(\kappa+1)}}\\&m_j=\frac{S_j^2-\beta^2-\alpha^2(\kappa+1)/(\kappa-1)}{2\beta-2(S_j+\beta)/(\kappa-1)}\quad j\in\{1,2,3,4\}\end{aligned}\tag{8}$$

In Eq. (7) and henceforth, subscripts $k\in\{1,2\}$ signify regions $0<y\le\eta$ and $\eta\le y<h$, respectively. The eight unknown coefficients $A_{kj}(\alpha)$ in Eq. (7) may be determined from boundary conditions (Eqs. (4) and (5)) in transformed space; their derivation is explained in the Appendix. Utilizing Hooke's law and Eq. (7), we arrive at stress components as

$$\sigma_{xxk}=\frac{2\mu_0 B_y e^{\beta(y+\eta)}}{\pi(\kappa+1)}\frac{(x-\xi)\left((y-\eta)^2-(x-\xi)^2\right)}{\left((y-\eta)^2+(x-\xi)^2\right)^2}+\frac{2\mu_0 B_x e^{\beta(y+\eta)}}{\pi(\kappa+1)}\frac{(y-\eta)\left(3(x-\xi)^2+(y-\eta)^2\right)}{\left((y-\eta)^2+(x-\xi)^2\right)^2}$$
$$-\frac{\mu_0 B_x e^{\beta(y+\eta)}}{\pi}\int_0^M\left\{\sum_{j=1}^4\left[\left(\frac{m_j(3-\kappa)(\beta+S_j)}{\alpha^2(\kappa-1)}-\frac{\kappa+1}{\kappa-1}\right)A_{kjE}e^{-S_j y}\right]+\frac{2(2-\alpha|\eta-y|)}{(\kappa+1)\operatorname{sgn}(y-\eta)}e^{-\alpha|y-\eta|}\right\}\cos(\alpha(x-\xi))d\alpha$$
$$-\frac{\mu_0 B_x e^{\beta(y+\eta)}}{\pi}\int_M^\infty\left\{\sum_{j=1}^4\left[\left(\frac{m_j(3-\kappa)(\beta+S_j)}{\alpha^2(\kappa-1)}-\frac{\kappa+1}{\kappa-1}\right)A_{kjE}e^{-S_j y}\right]-\left[\frac{2(2-\alpha|\eta-y|)}{(\kappa+1)\operatorname{sgn}(y-\eta)}+\frac{2\beta}{\alpha(\kappa+1)}\right]e^{-\alpha|y-\eta|}\right.$$
$$\left.+\frac{2\beta}{\kappa+1}\int_M^\infty\frac{1}{\alpha}e^{-\alpha|y-\eta|}\right\}\cos(\alpha(x-\xi))d\alpha$$
$$+\frac{i\mu_0 B_y e^{\beta(y+\eta)}}{\pi}\int_0^\infty\left\{\sum_{j=1}^4\left[\left(\frac{m_j(3-\kappa)(\beta+S_j)}{\alpha^2(\kappa-1)}-\frac{\kappa+1}{\kappa-1}\right)A_{kjO}e^{-S_j y}\right]+\frac{2(1-\alpha|\eta-y|)}{\kappa+1}e^{-\alpha|y-\eta|}\right\}\sin(\alpha(x-\xi))d\alpha$$

$$\sigma_{yyk}=\frac{2\mu_0 B_y e^{\beta(y+\eta)}}{\pi(\kappa+1)}\frac{(\xi-x)\left((x-\xi)^2+3(y-\eta)^2\right)}{\left((y-\eta)^2+(x-\xi)^2\right)^2}+\frac{2\mu_0 B_x e^{\beta(y+\eta)}}{\pi(\kappa+1)}\frac{(y-\eta)\left((y-\eta)^2-(x-\xi)^2\right)}{\left((y-\eta)^2+(x-\xi)^2\right)^2}$$
$$-\frac{\mu_0 B_x e^{\beta(y+\eta)}}{\pi}\int_0^M\left\{\sum_{j=1}^4\left[\left(\frac{m_j(\kappa+1)(\beta+S_j)}{\alpha^2(\kappa-1)}-\frac{3-\kappa}{\kappa-1}\right)A_{kjE}e^{-S_j y}\right]-\frac{2\alpha(\eta-y)}{\kappa+1}e^{-\alpha|y-\eta|}\right\}\cos(\alpha(x-\xi))d\alpha$$
$$-\frac{\mu_0 B_x e^{\beta(y+\eta)}}{\pi}\int_M^\infty\left\{\sum_{j=1}^4\left[\left(\frac{m_j(\kappa+1)(\beta+S_j)}{\alpha^2(\kappa-1)}-\frac{3-\kappa}{\kappa-1}\right)A_{kjE}e^{-S_j y}\right]-\left[\frac{2\alpha(\eta-y)}{\kappa+1}-\frac{2\beta}{\alpha(\kappa+1)}\right]e^{-\alpha|y-\eta|}\right. \quad (9)$$
$$\left.-\frac{2\beta}{\kappa+1}\int_M^\infty\frac{1}{\alpha}e^{-\alpha|y-\eta|}\right\}\cos(\alpha(x-\xi))d\alpha$$
$$+\frac{\mu_0 B_y e^{\beta(y+\eta)}}{\pi}\int_0^\infty\left\{\sum_{j=1}^4\left[\left(\frac{m_j(\kappa+1)(\beta+S_j)}{\alpha^2(\kappa-1)}-\frac{3-\kappa}{\kappa-1}\right)A_{kjO}e^{-S_j y}\right]+\frac{2(1+\alpha|\eta-y|)}{\kappa+1}e^{-\alpha|y-\eta|}\right\}\sin(\alpha(x-\xi))d\alpha$$

$$\sigma_{xyk}=\frac{2\mu_0 B_y e^{\beta(y+\eta)}}{\pi(\kappa+1)}\frac{(y-\eta)\left((y-\eta)^2-(x-\xi)^2\right)}{\left((y-\eta)^2+(x-\xi)^2\right)^2}-\frac{2\mu_0 B_x e^{\beta(y+\eta)}}{\pi(\kappa+1)}\frac{(x-\xi)\left((x-\xi)^2-(y-\eta)^2\right)}{\left((y-\eta)^2+(x-\xi)^2\right)^2}$$
$$-\frac{\mu_0 B_y e^{\beta(y+\eta)}}{\pi}\int_0^M\left\{\sum_{j=1}^4\left[\frac{i}{\alpha}(\beta+S_j-m_j)A_{kjO}e^{-S_j y}\right]-\frac{2\alpha(\eta-y)}{(\kappa+1)}e^{-\alpha|y-\eta|}\right\}\cos(\alpha(x-\xi))d\alpha$$
$$-\frac{\mu_0 B_y e^{\beta(y+\eta)}}{\pi}\int_M^\infty\left\{\sum_{j=1}^4\left[\frac{i}{\alpha}(\beta+S_j-m_j)A_{kjO}e^{-S_j y}\right]-\left[\frac{2\alpha(\eta-y)}{(\kappa+1)}+\frac{2\beta}{\alpha(\kappa+1)}\right]e^{-\alpha|y-\eta|}\right.$$
$$\left.+\frac{2\beta}{\kappa+1}\int_M^\infty\frac{1}{\alpha}e^{-\alpha|y-\eta|}\right\}\cos(\alpha(x-\xi))d\alpha$$
$$-\frac{\mu_0 B_x e^{\beta(y+\eta)}}{\pi}\int_0^\infty\left\{\sum_{j=1}^4\left[\frac{1}{\alpha}(\beta+S_j-m_j)A_{kjE}e^{-S_j y}\right]-\frac{2(1-\alpha|\eta-y|)}{(\kappa+1)}e^{-\alpha|y-\eta|}\right\}\sin(\alpha(x-\xi))d\alpha$$
$$k\in\{1,2\}$$

where *sgn*(.) is the sign function, M is an arbitrary constant, and A_{kjE}, A_{kjO} are the even and odd parts of $A_{kj}(\alpha)$, wherein $B_x=B_y=1$, with respect to parameter α. For the sake of computational convenience we take $0<M<1$, and also using the definition of the Exponential Integral, *Ei*(.), as

$$\int_M^{\infty} \frac{1}{\alpha} e^{-\alpha|y-\eta|} cos\left(\alpha\left(x-\xi\right)\right) d\alpha =$$
$$-\mathrm{Re}\left(Ei\left[\left(-|y-\eta|+i\left(x-\xi\right)\right)M\right]\right)$$
$$= -\gamma_0 - Ln\left(M\right) - Ln\left(\sqrt{\left(x-\xi\right)^2+\left(y-\eta\right)^2}\right) \quad (10)$$
$$-\sum_{k=1}^{\infty}\sum_{j=1}^{[k/2]} \frac{\left(-1\right)^j M^k \left(|y-\eta|\right)^{k-2j} \left(x-\xi\right)^{2j}}{k\left(2j\right)!\left(k-2j\right)!}$$

In Eq. (10), γ_0 is the Euler's constant, $Re(.)$ stands for the real part and $[k/2]$ is the largest integer $\le k/2$. From Eqs. (9) and (10), results that stresses fields are Cauchy as well as logarithmic singular in the dislocation position.

Due to analytical method of solution, some simplifications such as exponential variation of FGM properties or infinity of layer are inevitable. But these simplifications are very common [1-2], [4-8], and are not meaningless. For example if the crack has enough distance from the boundaries, effects of boundary on static SIFs of the crack is small. So, layer may be used to model cracked plate where cracks are not near the vertical boundaries. Furthermore effects of different functions on estimating property distributions of FGMs, on the static SIFs are relatively small [15].

For fracture analysis of a specific real problem, numerical solutions such as finite element method must be used. But analytical solutions may be used to benchmark the results obtained from numerical procedures. Furthermore, analytical solutions demonstrate effects of key parameters more easily.

3- Cracks Formulation

The preceding dislocation solution may be used to construct integral equations for analyzing strip with arbitrary oriented cracks. The stress components due to presence of an edge dislocation located at (ξ,η) are rewritten as

$$\sigma_{ij}\left(x,y\right) = \begin{cases} k_{ij}^{11}\left(x,y,\xi,\eta\right)B_x + k_{ij}^{12}\left(x,y,\xi,\eta\right)B_y & 0 < y \le \eta \\ k_{ij}^{21}\left(x,y,\xi,\eta\right)B_x + k_{ij}^{22}\left(x,y,\xi,\eta\right)B_y & \eta \le y < h \end{cases} \quad i,j \in \{x,y\} \quad (11)$$

where, $k_{ij}^{lm}, \{i,j\} \in \{x,y\}, \{l,m\} \in \{1,2\}$, are the coefficients of B_x and B_y in Eq. (9). Considering the layer be weakened by N cracks which may be described with respect to coordinate system x,y in parametric form as

$$x_i = \lambda_i\left(s\right), y_i = \chi_i\left(s\right), \qquad -1 \le s \le 1, \qquad i \in \{1,2,\ldots,N\} \quad (12)$$

A moveable orthogonal coordinate system n_s is chosen for ith crack such that n-axis is perpendicular to the crack surface. Suppose edge dislocations with unknown densities $b_{nk}(t)$ and $b_{sk}(t)$ are distributed on the infinitesimal segment $\sqrt{(\lambda'(t)^2+\chi'(t)^2)}\,dt$ at the surface of kth crack, where parameter $-1 \le t \le 1$ and the prime denotes differentiation with respect to the argument. The components of traction on the surface of ith crack results from distribution of dislocations on all N cracks yield

$$\sigma_{nni}(s) = \sum_{k=1}^{N}\int_{-1}^{1}\left\{K_{ik}^{11}(s,t)b_{sk}(t) + K_{ik}^{12}(s,t)b_{nk}(t)\right\}\sqrt{\lambda'(t)^2+\chi'(t)^2}\,dt$$
$$\sigma_{nsi}(s) = \sum_{k=1}^{N}\int_{-1}^{1}\left\{K_{ik}^{21}(s,t)b_{sk}(t) + K_{ik}^{22}(s,t)b_{nk}(t)\right\}\sqrt{\lambda'(t)^2+\chi'(t)^2}\,dt, \quad (13)$$
$$-1 \le s \le 1, \qquad i \in \{1,2,...,N\}$$

The kernels in integral Eq. (13) in terms of $k_{ij}^{lm}(.)$ in Eq. (11) may be found in [16].

By virtue of the Buckner's principal [17], the left-hand sides of Eq. (13) are applied traction on the presumed surface cracks with opposite sign. For the embedded cracks the unique solution to Cauchy singular integral Eq. (13) should satisfy the following closure requirements

$$\int_{-1}^{1}\left[\cos\left(\theta_k(1)-\theta_k(t)\right)b_{sk}(t) + \sin\left(\theta_k(1)-\theta_k(t)\right)b_{nk}(t)\right]\sqrt{\lambda'(t)^2+\chi'(t)^2}\,dt = 0$$
$$\int_{-1}^{1}\left[\cos\left(\theta_k(1)-\theta_k(t)\right)b_{nk}(t) - \sin\left(\theta_k(1)-\theta_k(t)\right)b_{sk}(t)\right]\sqrt{\lambda'(t)^2+\chi'(t)^2}\,dt = 0, \quad (14)$$
$$k \in \{1,2,...,N\}$$

In a cracked FGM body, stress fields near a crack tip exhibit the familiar square-root singularity. Therefore, dislocation densities are taken as

$$b_{lk}\left(t\right) = \frac{g_{lk}\left(t\right)}{\sqrt{1-t^2}}, \qquad -1 < t < 1, \qquad l \in \{s,n\}, \qquad k \in \{1,2,\ldots,N\} \quad (15)$$

Substitution of Eq. (15) into Eqs. (13) and (14) with application of the Gauss-Chebyshev quadrature scheme developed by Erdogan et al. [18] result in $g_{lk}(t)$, $l \in \{s,n\}$, $k \in \{1,2,\ldots,N\}$. Based on the definition of dislocation density function in terms of crack opening displacement, the mode I and II stress intensity factors, K_I and K_{II}, for an embedded crack may be expressed as

$$\begin{Bmatrix} K_{IIk} \\ K_{IIIk} \end{Bmatrix} = \frac{2\mu(y_{kL})\left[\lambda'(-1)^2+\chi'(-1)^2\right]^{1/4}}{1+\kappa}\begin{Bmatrix} g_{nk}(-1) \\ g_{sk}(-1) \end{Bmatrix}$$
$$\begin{Bmatrix} K_{IRk} \\ K_{IIRk} \end{Bmatrix} = -\frac{2\mu(y_{kR})\left[\lambda'(1)^2+\chi'(1)^2\right]^{1/4}}{1+\kappa}\begin{Bmatrix} g_{nk}(1) \\ g_{sk}(1) \end{Bmatrix}, \qquad k \in \{1,2,\ldots,N\} \quad (16)$$

Subscripts L and R designate the left and right tips of a crack.

4- Numerical Results

Due to lack of results about FG layers with fixed edges, the formulation is validated considering a central horizontal crack in a homogeneous layer, Fig. 2. For analysis of a homogeneous layer, gradation parameter β is set as a small value but not exactly zero in accordance to Eqs. (7) and (8). The Poisson's ratio of the layer is assumed $\upsilon=0$ and the plane strain state is considered. Crack is subjected to uniform normal traction. The variations of the normalized SIFs verses width of layer are compared with those obtained by Fichter [19] for the same problem which shows excellent agreement. To study effects of material nonhomogeneity on SIFs, the results for gradation parameter $2\beta h=3$ are also provided in Fig. 2. In homogenous case, due to symmetry of problem with respect to crack only mode I prevails. We observe that as width of layer decrease, which means the crack gets closer to fixed boundaries, mode I SIFs decrease significantly. Due to material asymmetry in nonhomogenous case, mode II SIFs exist which have opposite signs in left and right tips of crack. In following examples to ensure the opening of cracks, the layer is under constant biaxial traction σ on the edges and at the far-field as $|x| \to \infty$ which results normal traction σ on crack surfaces. Furthermore, plane strain condition is assumed and Poisson's ratio is $\upsilon=0.3$. As the second example, a FG layer with a central rotating crack around its center with normalized lengths $2l=0.6$ is considered. Variation of

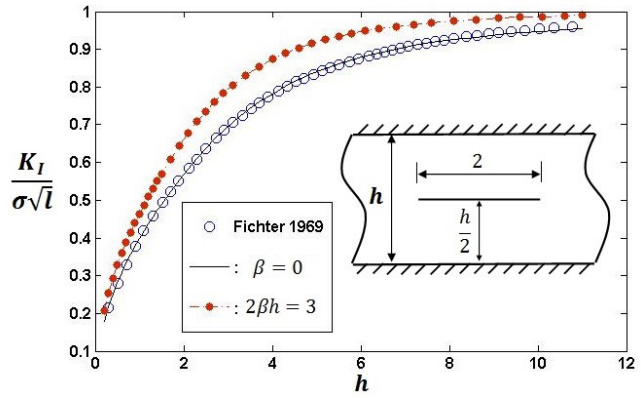

(a)

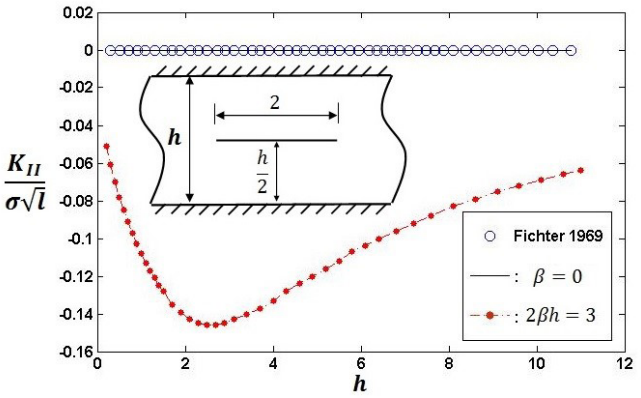

(b)

Fig. 2. Variation of normalized SIFs verses width of layer

SIFs verses orientation of crack is shown in Fig. 3 for three different values of gradation parameter β. As expected, it is observed that in horizontal case, θ=0, mode *I* SIFs of left and right tips of crack are equal and mode *II* SIFs have opposite signs. Furthermore, in vertical case, θ=90, mode *II* SIFs vanish due to symmetry considerations. In FGM layer, it is observed that SIFs for crack tip *R* which is located in stiffer region is larger than SIFs of crack tip *L*. Effect of gradation parameter β on trends of variations of SIFs is not strong but affects their values.

To show effect of fixed boundaries more clearly, SIFs

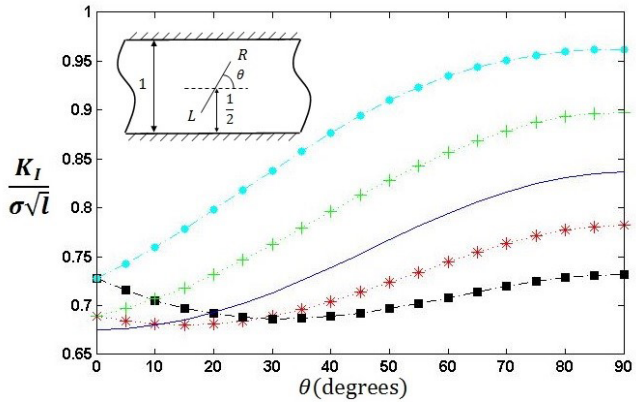

(a)

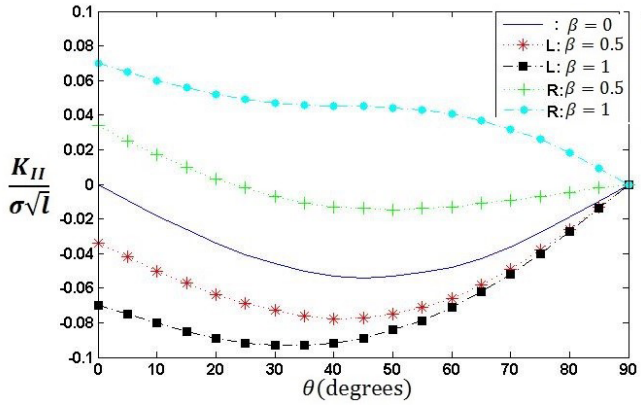

(b)

Fig. 3. SIFs for a central rotating crack

of an off-center rotating crack are depicted in Fig. 4. In homogenous case, β=0, mode *I* SIFs of crack tip *L*, which is located farther from boundary, is greater than crack tip *R*. In FGM layer with exponent β=0.5, for angle of rotation larger than θ~65°, effects of fixed boundary conditions dominate and mode *I* SIFs of crack tip *L* gets larger than tip *R*. But for FGM parameter β=1, effect of gradation of material is stronger which causes SIFs of crack tip *R* being larger than tip *L* for all values of θ. Comparing mode *II* SIFs in Figs. 3 and 4, shows effects of asymmetry of boundary conditions which causes larger SIFs for off-center crack.

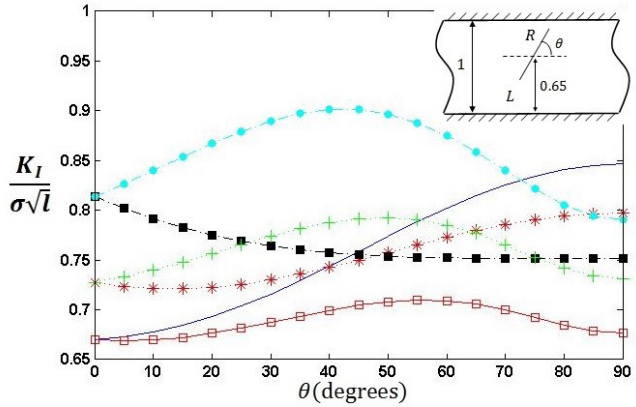

(a)

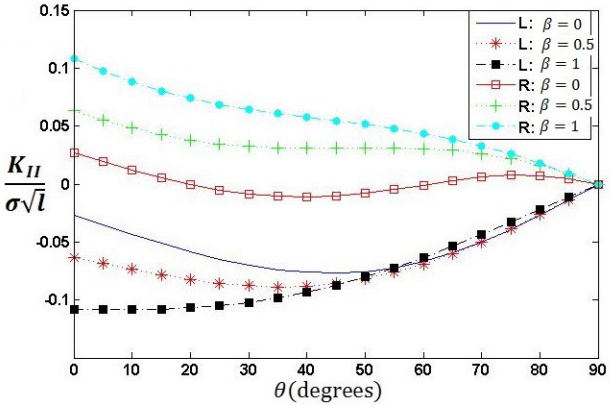

(b)

Fig. 4. SIFs for an off-center rotating crack

As the next example, we consider a FG layer with two cracks, one stationary and a rotating crack around its center, with normalized lengths $2l$=0.6. Fixed crack is horizontal and centers of both cracks are in the mid of the layer. Normalized SIFs verses different orientation of rotating crack is shown in Fig. 5 for two different values of FGM exponent β. As expected, at θ=0, i.e., the case of horizontal cracks, mode *I* SIFs of tips L_1 and R_1 are equal to those at R_2 and L_2 respectively. It is observed that the variation of β has minor effects on trends of SIFs except on tip L_2 which is influenced by interaction of cracks and material gradation simultaneously. Mode *I* SIFs at right tip of rotating crack, R_2, which has weak interaction with fixed crack, increases greatly with increasing β due to the fact that the crack tip lies in the comparatively stiffer location.

As the last example, the interaction of two fixed vertical cracks and a horizontal crack with variable location is considered. The lengths of cracks are $2l$=0.4. The mode *I* and *II* SIFs of cracks verses distance d for two different values of β are shown in Fig. 6. Due to the symmetry considerations, vertical cracks have the same SIFs; besides, SIFs at crack tips L_2 and R_2 are equal. In homogenous case, β=0, mode *I* SIFs of crack tip L_2 is symmetric and values of SIFs at crack tips L_1 and R_1 interchange as horizontal cracks passes to the other side of layer central line. The variation of mode *I* SIFs for both materials manifest the same trend except for crack tip L_2 which results from variation of its location and material gradation. Interaction between cracks causes magnification of mode *I* SIFs at tips L_1 and R_1. Furthermore, shielding phenomena at tip L_2 is observed.

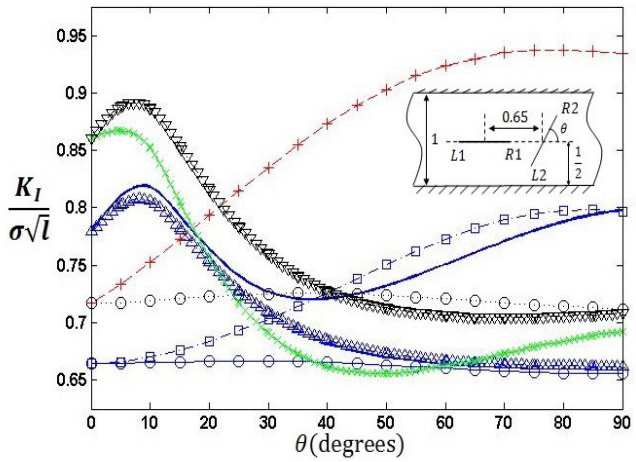

(a)

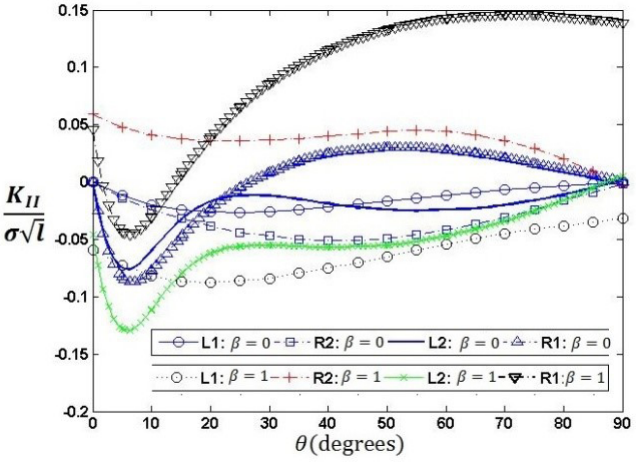

(b)

Fig. 5. SIFs for a stationary and a rotating cracks

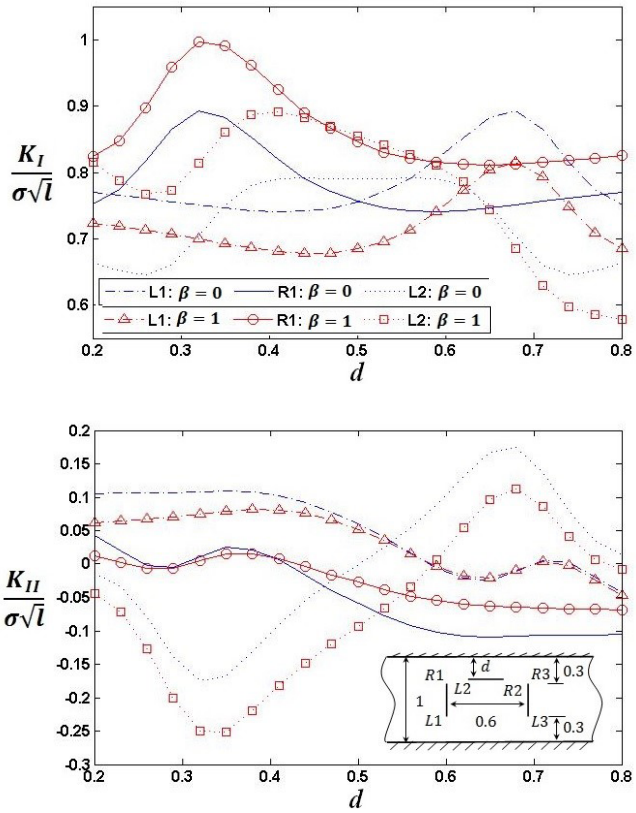

Fig. 6. SIFs for a variable location horizontal and two fixed vertical cracks

5- Conclusions

The solution of an edge dislocation in a FGM layer with fixed longitudinal boundaries is obtained. The distributed dislocation technique is utilized to derive integral equations for analyzing a layer weakened by multiple cracks. Effects of fixed boundary conditions on SIFs and their dependency on the material gradation parameter are studied for different configuration of cracks. Cracks are assumed under normal traction, thus mode *II* SIFs results from gradation of material or interaction of cracks and their values were smaller than mode *I* SIFs. It is observed that cracks closer to the boundary experience lower SIFs values in contrast to usual free boundary conditions. Furthermore, in general, crack tips located in a region with higher shear modulus, have larger SIFs. We also found that gradation parameter has weak effects on trends of variation of SIFs but affects their values, as it is expected. Several solved examples illustrate clearly the competing effects of cracks configuration, material nonhomogeneity and boundary condition on the SIFs.

Acknowledgement

The first author acknowledges the funding support of Babol Noshirvani University of Technology through grant program

No. BNUT/394096/98.

Appendix

The coefficients $A_{ij}(\alpha)$ in Eq. (7) are obtained from the following equation

$$X = D^{-1}F \tag{17}$$

where, vectors X,F and nonzero elements of matrix D are

$$\begin{aligned}
&D_{1(2j-1)} = -e^{-S_j\eta} \quad , \quad D_{1(2j)} = e^{-S_j\eta} \quad , \quad j \in \{1,2,3,4\} \\
&D_{2(2j-1)} = i\,m_j e^{-S_j\eta}/\alpha \quad , \quad D_{2(2j)} = -i\,m_j e^{-S_j\eta}/\alpha \quad , \quad j \in \{1,2,3,4\} \\
&D_{3(2j-1)} = (\beta+1)e^{-S_j\eta} \quad , \quad D_{3(2j)} = -(\beta+1)e^{-S_j\eta} \quad , \quad j \in \{1,2,3,4\} \\
&D_{4(2j-1)} = -i(\beta+1)m_j e^{-S_j\eta}/\alpha \quad , \quad D_{4(2j)} = i(\beta+1)m_j e^{-S_j\eta}/\alpha \quad j \in \{1,2,3,4\} \\
&D_{5j} = 1 \quad , \quad D_{6j} = m_{(j+1)/2} \quad , \quad j \in \{1,3,5,7\} \\
&D_{7j} = e^{-S_j/2h} \quad , \quad D_{8j} = m_{j/2}e^{-S_j/2h} \quad , \quad j \in \{2,4,6,8\}
\end{aligned} \tag{18}$$

$$F_{11} = B_x \quad , \quad F_{21} = B_y \quad , \quad F_{31} = i\alpha B_y \quad , \quad F_{41} = i\alpha\frac{3-\kappa}{\kappa+1}B_x$$

References

[1] F. Erdogan, B. Wu, The surface crack problem for a plate with functionally graded properties, *Journal of applied Mechanics*, 64(3) (1997) 449-456.

[2] S. Kadioğlu, S. Dag, S. Yahsi, Crack problem for a functionally graded layer on an elastic foundation, *International Journal of Fracture*, 94(1) (1998) 63-77.

[3] Z.-H. Jin, G.H. Paulino, A viscoelastic functionally graded strip containing a crack subjected to in-plane loading, *Engineering Fracture Mechanics*, 69(14-16) (2002) 1769-1790.

[4] L.-C. Guo, L.-Z. Wu, L. Ma, T. Zeng, Fracture analysis of a functionally graded coating-substrate structure with a crack perpendicular to the interface-Part I: Static problem, *International Journal of fracture*, 127(1) (2004) 21-38.

[5] X. Long, F. Delale, The general problem for an arbitrarily oriented crack in a FGM layer, *International journal of fracture*, 129(3) (2004) 221-238.

[6] X. Long, F. Delale, The mixed mode crack problem in an FGM layer bonded to a homogeneous half-plane, *International Journal of Solids and Structures*, 42(13) (2005) 3897-3917.

[7] S. El-Borgi, R. Abdelmoula, S. Dag, N. Lajnef, A surface crack in a graded coating bonded to a homogeneous substrate under general loading conditions, *Journal of Mechanics of Materials and Structures*, 2(7) (2007) 1331-1353.

[8] S. Dag, B. Yildirim, D. Sarikaya, Mixed-mode fracture analysis of orthotropic functionally graded materials under mechanical and thermal loads, *International Journal of Solids and Structures*, 44(24) (2007) 7816-7840.

[9] Z. Zhong, Z. Cheng, Fracture analysis of a functionally graded strip with arbitrary distributed material properties, *International Journal of Solids and Structures*, 45(13) (2008) 3711-3725.

[10] Z. Cheng, D. Gao, Z. Zhong, Interface crack of two dissimilar bonded functionally graded strips with arbitrary distributed properties under plane deformations, *International Journal of Mechanical Sciences*, 54(1) (2012) 287-293.

[11] M. Ben-Romdhane, S. El-Borgi, M. Charfeddine, An embedded crack in a functionally graded orthotropic coating bonded to a homogeneous substrate under a frictional Hertzian contact, *International Journal of Solids and Structures*, 50(24) (2013) 3898-3910.

[12] V. Petrova, S. Schmauder, Modeling of thermomechanical fracture of functionally graded materials with respect to multiple crack interaction, *Physical Mesomechanics*, 20(3) (2017) 241-249.

[13] L. Guo, S. Huang, L. Zhang, P. Jia, The interface crack problem for a functionally graded coating-substrate structure with general coating properties, *International Journal of Solids and Structures*, (2018).

[14] M. Monfared, R. Bagheri, R. Yaghoubi, The mixed mode analysis of arbitrary configuration of cracks in an orthotropic FGM strip using the distributed edge dislocations, *International Journal of Solids and Structures*, 130 (2018) 21-35.

[15] B. Wang, Y.-W. Mai, N. Noda, Fracture mechanics analysis model for functionally graded materials with arbitrarily distributed properties, *International Journal of Fracture*, 116(2) (2002) 161-177.

[16] A. Fotuhi, S. Fariborz, Stress analysis in a cracked strip, *International Journal of Mechanical Sciences*, 50(2) (2008) 132-142.

[17] H. Bueckner, The propagation of cracks and the energy of elastic deformation, *Transaction of the ASME, Series E*, 80(6) (1958) 1225-1230.

[18] F. Erdogan, G.D. Gupta, amp, T. Cook, *Numerical solution of singular integral equations, in: Methods of analysis and solutions of crack problems*, Springer, 1973, pp. 368-425.

[19] W.B. Fichter, *Stresses at the Tip of a Longitudinal Crack in a Plate Strip*, (1967).

Please cite this article using:

A.M. Baghestani and S.J. Fariborz, Mixed-Mode Fracture Analysis of a Functionally Graded Layer with Clamped Longitudinal Edges, *AUT J. Mech. Eng.*, 3(2) (2019) 235-242.

DOI: 10.22060/ajme.2019.14844.5748